Solid State Ionics 32/33 (1989) 314–329
North-Holland, Amsterdam

ALBITE FELDSPAR HYDROLYSIS TO 300°C

Roland HELLMANN*, David A. CRERAR
Department of Geological and Geophysical Sciences, Princeton University, Princeton, N.J. 08544, USA

and

Ronghua ZHANG
Institute of Mineral Deposits, Chinese Academy of Geological Sciences, Beijing, P.R. China

Received 31 May 1988; accepted for publication 19 August 1988

The dissolution of albite in aqueous solutions at temperatures ranging from 25 to 300°C and *pH*'s from 2.4 to 10.1 was investigated by determining the stoichiometric ratios of Al/Si, Na/Si and Al/Na in the effluent solution. The experiments were carried out in a tubular plug flow reactor. The solution data collected at temperatures above 100°C were representative of steady state dissolution behavior. Under these conditions, both the Al/Si and the Na/Si ratios showed negative incongruency. The deficiency of Al was attributable to the observed precipitation of a crystalline boehmite (AlO(OH)) reaction rim. The high porosity of the boehmite phase prevented it from behaving as a diffusional barrier to the outward flux of Si from the structure. The deficiency of Na was much less than that of Al, and was probably due to the sorption of Na ions either at the feldspar–boehmite interface and/or within the boehmite. If these factors are taken into account, then it can be assumed that steady state dissolution is congruent. At temperatures of 25 and 100°C, the Al/Si and Na/Si ratios generally showed positive incongruency, indicating the preferential release of Al and Na with respect to Si. This reveals that the initial, non-steady state phase of dissolution leads to a leached near-surface zone which is depleted in Na and Al. This altered layer is probably not uniform in depth or lateral extent since there was evidence for preferential attack of the feldspar at specific sites on the surface, leading to etch pit formation. When the low temperature, non-steady state results are taken together with the high temperature, steady state results, then the hydrolysis of feldspars can be considered to be a two-step process: first, there is the initial development of a non-uniform leached zone due to incongruent dissolution; the subsequent steady state, stoichiometric dissolution process occurs when the rate of diffusion of product ions through the leached zone equals the rate of structure breakdown.

1. Introduction

1.1. Rock-water interactions and feldspars

The chemical and physical evolution of many geological systems is a function of rock–water interactions. Equilibrium solubility studies are useful in assessing the final state of any particular rock–water system, thus allowing for the prediction of which phases should dissolve and which others will eventually precipitate. However, in many cases, geological systems are constrained by conditions where irreversible thermodynamic processes, which have never attained true equilibrium, predominate. The ability to predict how such rock–water systems will evolve over time then becomes a question of the kinetics of the chemical and physical reactions occurring within such systems.

Any rock–water system is inherently complex due to the large number of components and variables present. Therefore, it becomes necessary to decompose the problem into an investigation of the individual hydrolysis reactions of the component minerals. Feldspars are the most common occurring

* Address after 1 December 1988: Université Paul Sabatier – CNRS, Laboratoire de Mineralogie et Cristallographie, 38, Rue des Trent-six Ponts, 31400 Toulouse, France.

silicates in the near-surface of the crust, where they occur in a wide variety of geological environments. The hydrolysis reaction(s) of feldspars can be particularly difficult to study experimentally due to complexities associated with incongruent dissolution behavior. Thus, before rate constants for such reactions can be determined, the exact nature of the dissolution process must first be adequately understood. For the purposes of this study we have chosen albite ($NaAlSi_3O_8$), a feldspar belonging to the plagioclase feldspar solid solution series ($NaAlSi_3O_8$–$CaAl_2Si_2O_8$). In this study the behavior of albite dissolution was investigated over conditions ranging from those at the surface of the earth to shallow hydrothermal environments, where temperatures generally do not exceed 300°C.

Since feldspars are such a ubiquitous mineral component of so many rock types, information gained from dissolution studies will yield important information on the overall dissolution behavior of a large number of rock types. In a very broad sense, these types of experiments will yield much of the needed information to more fully understand many of the fundamental problems of geochemistry and petrology related to the flow of aqueous solutions through crustal rocks. In addition to the earth sciences, rock–water studies have also found broad application in the development of in situ mining techniques, radwaste burial leaching studies, geothermal power generation and ground water contaminant flow modeling.

1.2. Hydrolysis models and this study

Current feldspar hydrolysis models fall into two broad categories. The diffusion-limited model is based on the hypothesis that diffusion through secondary surface layers controls the outward flux of dissolution products. This model is based on data from experiments conducted under a variety of conditions, which showed that product ions were not released in their stoichiometric proportions (see, for example: Correns and von Engelhardt [1], Wollast [2], Tsuzuki and Suziki [3] and references therein). The incongruency of feldspar dissolution, particularly with respect to the deficiency of Al in solution, was thought to be caused by the precipitation of "armoring" precipitates, such as kaolinite, muscovite, montmorillonite and boehmite. The type of precipitate was found to be a function of the compositions of the fluid and the solid. Another variation of the diffusion model is based on the hypothesis that a thin leached zone forms at the near surface of the solid, due to the rapid exchange of protons for alkalis within the lattice (Garrels and Howard [4], Pačes [5], Chou and Wollast [6,7], Wollast and Chou [8], Holdren and Speyer [9] and references therein). According to this model, the reaction becomes congruent when the leached zone attains a steady state thickness; this occurs when the rate of dissolution equals the rate of diffusion through the layer. Despite solution data supporting this hypothesis, surface spectroscopy data have not supported this idea (Petrović et al. [10], Holdren and Berner [11] and Fung et al. [12]).

In contrast to the diffusion model, the surface reaction model invokes a surface control mechanism where congruent dissolution at specific activated sites on the surface is the rate controlling step. This hypothesis is supported by evidence that surface area has been found to be generally proportional to the rate of reaction; SEM micrographs showing etch pit development also support this model (Lagache [13,14], Berner and Holdren [15], Aagaard and Helgeson [16], Helgeson et al. [17], Dibble and Tiller [18], Berner and Schott [19], Berner et al. [20], Holdren and Speyer [21], Knauss and Wolery [22] and references therein). It was recently proposed that the leached layer model be modified such that the formation of leached zones is not uniform, but rather localized at sites of high surface strain energy (Chou and Wollast [23] and Berner et al. [20]).

Even though there have been a large number of studies on the hydrolysis of feldspars, most of them have been restricted to temperatures below 100°C. The few studies that were done at higher temperatures were virtually all carried out in batch reactors. One of the limitations of batch experiments is that changing the input solution necessitates the disruption of the run. The other drawback of batch reactors is that the chemical affinity of the hydrolysis reaction continuously changes with time; this can complicate the correct interpretation of the data. Experiments utilizing flow reactors are generally much less time consuming since the input solution chemistry can be changed without having to disrupt the ex-

periment. In addition to this, for any given constant experimental conditions, the chemical affinity of the reaction remains invariant with time. In the case of tubular reactors, an axial chemical gradient can exist, depending on the axial length of the reactor and the rate of reaction. Nevertheless, any gradients which do occur are constant under steady state conditions.

The study reported here is one of the first to utilize a flow system to measure the dissolution of feldspars at temperatures to 300°C. The main goal was to investigate the aqueous stoichiometries of the reaction products, as measured by the ratios of Al/Si, Na/Si and Al/Na in the reactor effluent. The measurements were made both at steady state and non-steady state conditions. By doing so, information on the mechanism of dissolution could be elucidated for the initial phases of dissolution and the subsequent steady state stage. We also carefully characterized the surfaces both before and after reaction.

2. Experimental design and methods

2.1. Preparation and characterization of samples and solutions

For these experiments we used Amelia albite since it is one of the "purest" albites commercially available; it has also been well characterized in the mineralogical literature. The experiments were run using crushed grains (0.18–0.15 mm) from which extraneous phases, such as quartz, micas and magnetic minerals, had been previously separated. Grains were then treated ultrasonically in acetone for 1/2 hour to remove surface fines. The homogeneity of the sample was then checked both by X-ray diffraction (XRD) of a powder as well as by electron microprobe analyses of a polished section. After sonification, surface area determinations were made of representative samples using the single point BET technique.

Input solutions were made from deionized water; based on *pH* measurements the water used was in equilibrium with atmospheric CO_2. Acidic and basic solutions were prepared with HCl and NaOH, respectively. In all cases *pH* buffers were not used in order to eliminate possible interferences by the buffering compounds. The solution *pH*'s were continuously monitored over the course of each experiment and were found to be quite steady (± 0.05).

2.2. Flow system design, methodology and conditions

The experiments were run in a flow system using a vertically mounted tubular plug flow reactor. The system was constructed almost entirely of titanium to limit corrosion. Input solutions were pumped through the system with an HPLC pump in a one-pass flow mode. To ensure that the fluid was at the proper experimental temperature, solutions first passed through a preheating column before contacting the packed bed of feldspar in the reactor. The feldspar grains (runs utilized approximately 9 g) were held in place within the reactor by titanium frits. Solutions, upon exiting the reactor and the furnace, cooled down before they passed through the back pressure regulator and were sampled. The regulator maintained the system pressure at a constant value of 170 Bars. In all cases, experiments were run at pressures exceeding vapor saturated water pressure. Fig. 1 shows a schematic diagram of the flow system. Further details of the apparatus used can be found in Posey-Dowty et al. [24].

The experiments were run under a wide variety of conditions. Temperatures ranged from 25 to 300°C, *pH*'s were varied from 2.46 to 10.12 and flow rates spanned a range from 0.7 to 2.9 ml/min (commensurate to average residence times of 4.4 to 1.3 min, respectively). The flow through the reactor bed was non-turbulent. Based on calculations incorporating variable flow rates and temperatures (which affects the viscosity), the particle Reynolds number (N_{Re}) was on the order of 0.01 to 1.

The packed bed experiments generally lasted from 500 to 600 h each. During the course of an experiment, three variables were continually changed: flow rate, temperature and input *pH*. These variables are listed in order of their hierarchy, i.e., for any given input *pH*, samples were obtained for temperatures ranging from 25 to 300°C, and at any given temperature, samples were taken at various flow rate settings. At the start of a new experiment, the packed bed was exposed to flowing water at 25°C for 24 h in order to eliminate, as much as possible, any re-

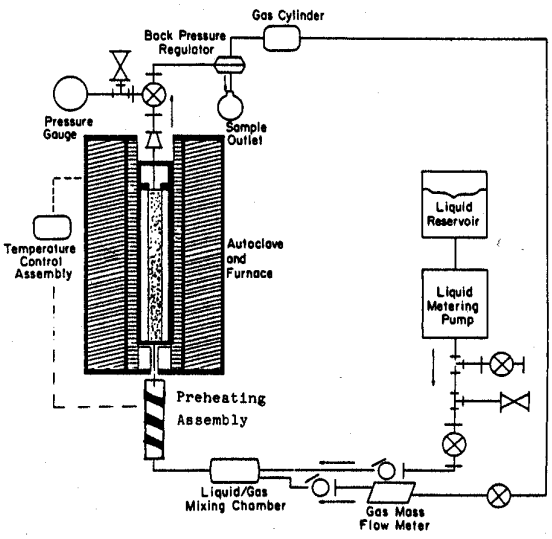

Fig. 1. A schematic diagram of the flow system used in this study. Solutions were pumped with an HPCL pump through a preheating chamber before contacting the crushed mineral bed residing in the tubular reactor. Output solutions were sampled downstream from the back pressure regulator. The liquid–gas mixing chamber was not utilized for this set of experiments. Virtually all wetted parts of the flow system were made of titanium. Adapted from ref. [24].

sidual surface fines adhering to the grains. After the initial conditioning period, samples of the output solution were taken for a variety of flow rate settings. The time allowed for dynamic equilibrium to be reached between each flow setting ranged from 1/2 to 4 h, depending on the flow rate. Temperature settings were incrementally changed in the following order: 25, 100, 175, 225, 300, 25°C. The temperature setting was brought back down to 25°C to check the repeatability of the results. Approximately 2 1/2 h were allowed for chemical equilibration once a particular new temperature setting had been reached. When changes in solution *pH* were made, 24 h were allowed to pass (at 25°C) before sampling was resumed. Exposure of the grains to high temperatures, where the dissolution rate is highest, was kept to a minimum to minimize changes in the characteristics of the grains (such as surface area, etc.) during the course of an experiment. The first series (#1) of experiments used input solutions with *pH*'s of (in experimental order) 2.46, 3.21, 5.45 and 5.7; the second series (#2) of experiments used solutions with *pH*'s 5.7, 10.12, 9.16 and 5.7.

Samples were collected in triplicate. After their *pH*'s were measured, the solutions were acidified with HCl prior to analysis for Al, Na and Si. At concentrations greater than 500 ppb, solution analyses were made using inductively coupled plasma spectrophotometry (ICP–ES). At lower concentrations, Si was measured colorimetrically using the silicomolybdate blue method described by Strickland and Parsons [25], and Al and Na were measured by atomic absorption (AA) techniques (graphite furnace AA and flame AA, respectively). At concentrations greater than 500 ppb, we estimated that our analytical accuracy was in the range of 5–10%; this figure rose to 10–15% for all methods at low concentrations.

3. Results

3.1. Release ratios

The data collected from experimental series 1 and 2 are shown in graphical form (figs. 2–4) in terms of Al/Si, Na/Si and Al/Na release ratios. The release ratios were measured at 25, 100, 225 and 300°C. The data have been spread apart on each plot, such that the dependence on input *pH* is also shown. At each temperature and *pH*, compositions were measured in triplicate at several flow rates; each graphical symbol represents one analysis. A particular release ratio is a measure of the stoichiometric ratio of one element to another element in solution, normalized to their stoichiometric ratio in the solid. Based on weight percentages, ten microprobe analyses of a polished section of Amelia albite yielded the following solid stoichiometric ratios and corresponding values for 1σ: $Na/Si = 0.288 \pm 0.005$; $Al/Si = 0.358 \pm 0.004$; $Al/Na = 1.243 \pm 0.023$. Release ratios can be used to decipher key aspects of the hydrolysis of the structure, provided that the release ratio attributable to the actual breakdown of the structure has not been altered by any secondary processes which may selectively retain one or more product species. An example of such a process would be the precipitation of a secondary phase.

Relative release ratios are defined ([9]) as follows (based on Si):

$$\log(rrr)_X = \log \frac{(X/Si)_{aq}}{(X/Si)_{solid}}, \quad (1)$$

where X = Na or Al.

Release ratios are by definition dimensionless. The units chosen for the numerator and the denominator must be equivalent for the ratio to be meaningful. The sign of the release ratio is indicative of whether dissolution is congruent or incongruent. The equations below summarize the three variations that the release ratio can assume:

$$\log(rrr)_X = 0: \frac{dX}{dt} = \frac{dSi}{dt}; \text{congruent}, \quad (2)$$

$$\log(rrr)_X > 0: \frac{dX}{dt} > \frac{dSi}{dt}; (+) \text{ incongruency}, \quad (3)$$

$$\log(rrr)_X < 0: \frac{dX}{dt} < \frac{dSi}{dt}; (-) \text{ incongruency}. \quad (4)$$

3.2. Experimental results

3.2.1. Aluminum/silicon

Fig. 2 shows the release ratios of Al/Si from the data of series 1 and 2. Despite the large amount of scatter in the data at lower temperatures (25 and 100°C), it is apparent that the means of the release ratios change from positive to negative over the range of 25 to 100°C. This indicates that at 25°C Al is preferentially released into solution with respect to Si. The degree of preferential release of Al is quite substantial since the means of the release ratios lie in the range of 0 to +1.5 log units. At temperatures of 100°C and above, the means of the release ratios are in the range of 0 to −3.0 log units, indicating that Al is preferentially retained.

The data for temperatures of 175°C and above also

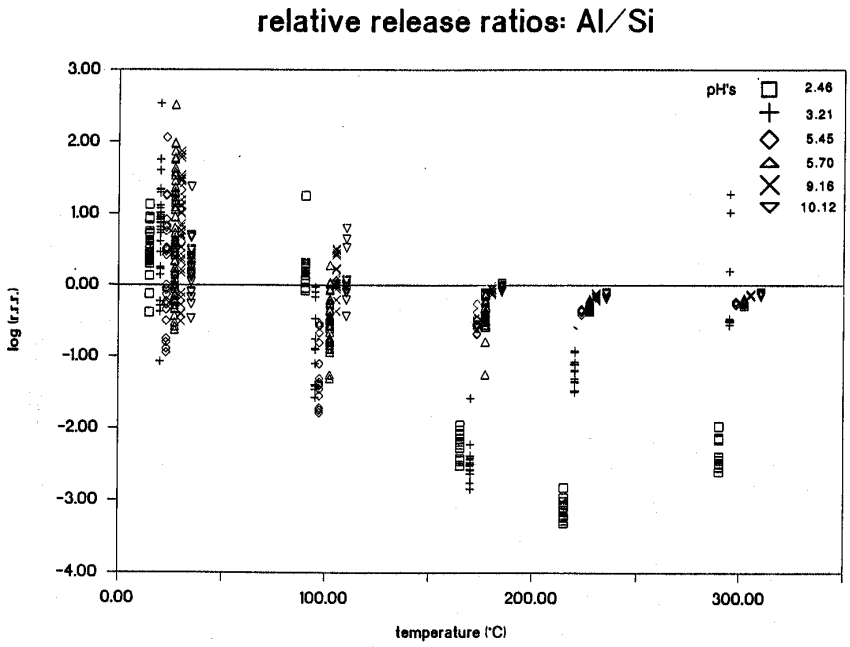

Fig. 2. The relative release ratios for Al/Si, Na/Si and Al/Na as a function of temperature and *pH*. Release ratios were measured at 25, 100, 175, 225 and 300°C. The data have been spread apart at each temperature to show the dependence of the ratios on *pH*. At each temperature and *pH*, compositions were measured in triplicate at several flow rates; each symbol represents one analysis. Positive release ratios represent the preferential release of a given component (the numerator of the ratio) into solution, and conversely, negative values represent preferential retention.

show that the release ratios, for any given temperature, vary as a function of input *pH*. As an example, at 225°C the mean of the release ratios at pH_{in} 2.46 is approximately −3.0. At a pH_{in} of 3.21, the mean of the release ratios is much higher, approximately −1.2. The sharp increase in the values of the release ratios with increasing pH_{in} becomes much less pronounced at intermediate to high *pH*'s (5.45–10.12). At these *pH*'s, the means of the release ratios fall in the narrow range of −0.5 to −0.1. These trends indicate that the degree of Al retention at temperatures above 100°C is inversely dependent on pH_{in}, with the highest degree of preferential Al retention occuring at the lowest pH_{in}.

3.2.2. Sodium/silicon

Fig. 3 shows the release ratio data for Na/Si. In many respects, the trends are quite similar to those observed previously for Al/Si in fig. 2. At 25 and 100°C, the means of release ratios plot within the positive incongruency field, indicating that Na is preferentially released into solution in comparison to Si. At 175°C, most of the release ratio means plot either on the congruency line, or within one or two tenths of a log unit from it. At higher temperatures (225 and 300°C), the means of the data are tightly clustered between 0 and −0.15 log units, indicating slight negative incongruency. This is indicative of the preferential retention of Na. The degree of Na retention at high temperatures is, however, several orders of magnitude less than Al, especially at low *pH*'s. In contrast to the Al/Si results, there does not appear to be any significant relation between input *pH* and the value of the release ratio for any given temperature.

3.2.3. Aluminum/sodium

Based on the Al/Si and Na/Si release ratio trends, the Al/Na trends are easily predictable in advance. Fig. 4 shows that virtually all of the means lie within the negative incongruency field. As was the case with the Al/Si and Na/Si plots, there is a considerable degree of scatter in the data at low temperatures. Nevertheless, even at low temperatures (25 and 100°C), it is apparent that either Al is preferentially retained with respect to Na, or conversely, Na per-

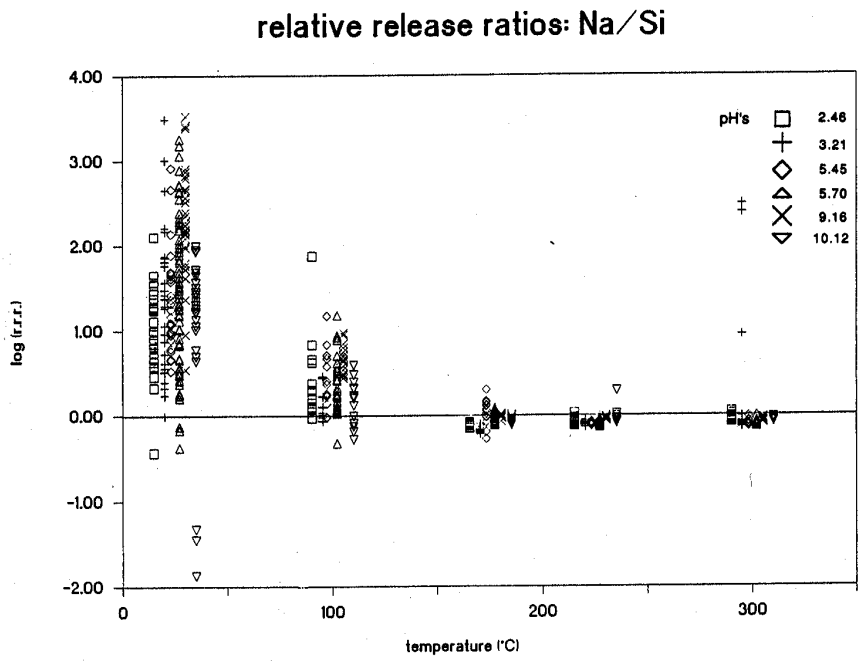

Fig. 3. The same as fig. 2.

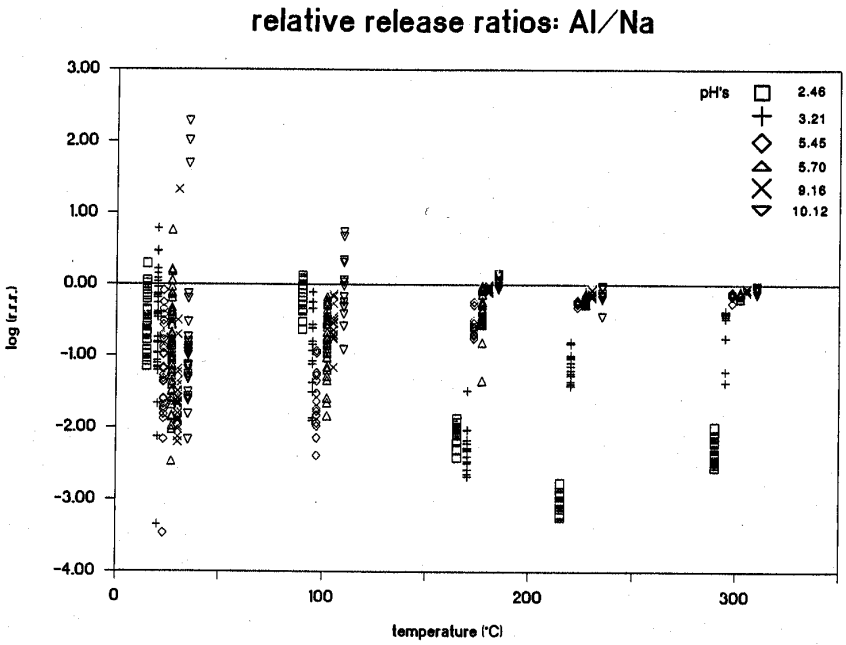

Fig. 4. The same as fig. 2.

haps is released at a faster rate than Al. At temperatures above 100°C, the means of the data are much more tightly clustered for any given pH_{in}. It is also apparent that at these temperatures there exists a negative dependency between the pH_{in} and the release ratio. The trend observed in fig. 4 closely resembles, as expected, the *pH*-release ratio trend for Al/Si. This suggests that Al is always preferentially retained at low *pH*'s and high temperatures, both with respect to Na and Si.

3.2.4. Flow rate dependence and reproducibility results

Based on figs. 2–4, two of the three experimental parameters, *T* and *pH*, which were varied during the course of each run, have a significant effect on the value of the release ratios of Al/Si, Na/Si and Al/Na. The third parameter, flow rate, was not separately considered since we found that when release ratio plots were constructed as a function of residence time, holding temperature and pH_{in} constant, no observable trends were apparent for Na/Si release ratios. In some cases, there was a small dependency of the Al/Si release ratios on residence time at *pH* 2.46, such that the means of the ratios decreased up to one tenth of a log unit from the lowest to the highest residence time. If this effect is real, then it would indicate that Al retention is favored by slower flow rates. However, this effect was judged too small, relative to the dependence on temperature and pH_{in}, to warrant the separate treatment of flow rates and release ratios.

In order to determine whether the release ratios were reproducible, a comparison was made between data from experimental series 1 and 2 at a pH_{in} of 5.7, this being the only *pH* both series had in common. Figs. 5 and 6 show that at all temperatures, the degree of reproducibility in terms of the Al/Si and Na/Si release ratios was very good. At low temperatures, the degree of scatter was considerable in both cases. At temperatures above 100°C, the means of the release ratios were within one to two tenths of a log unit within each other. An internal comparison was also made of the data from series 2. In this case, the experiment commenced and ended with solutions of $pH_{in} = 5.7$. This afforded a comparison be-

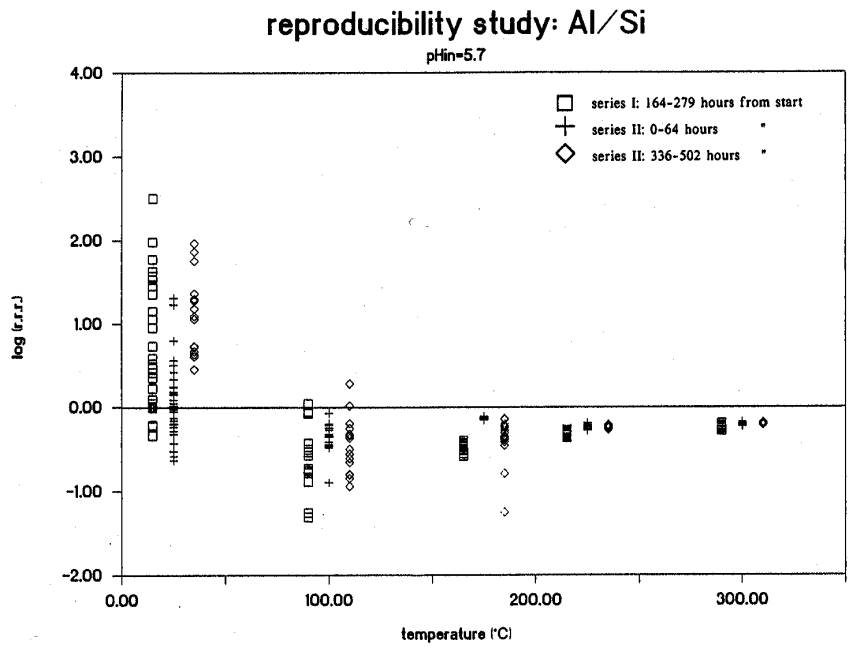

Fig. 5. The reproducibility measurements for Al/Si and Na/Si release ratios allow for the comparison of data at a pH_{in} of 5.7, both between experiments of series 1 and 2, as well as within series 2. The agreement between the data is quite good, particularly at temperatures above 100°C.

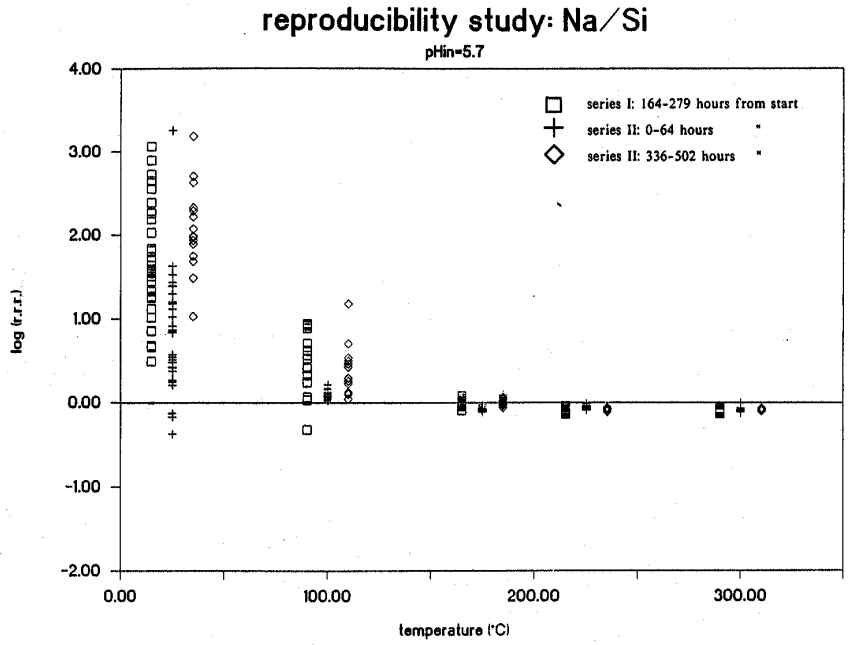

Fig. 6. The same as fig. 5.

tween release ratios obtained at the beginning of the experiment (0–64 h) with those obtained at the end (336–502 h). In this case, as well, there were no significant differences.

4. Discussion

4.1. Preferential aluminum retention above 100°C

As fig. 2 shows, the Al/Si release ratios were negative at temperatures exceeding 100°C. This suggests that Al was being preferentially retained, especially at very low *pH*'s. In order to test this hypothesis, we subjected large albite cleavage fragments (several mm on a side) to input solutions of *pH* 2.36 at 300°C for periods ranging from 24 to 80 h. Under these conditions a white, friable secondary precipitate formed a rind around each albite fragment. An X-ray diffraction pattern (using Cu Kα radiation) yielded a very definitive boehmite pattern (AlO(OH)), as can be seen in fig. 7. No other phases could be positively identified on the X-ray diffraction pattern. Microprobe traverses from the albite-boehmite interface across the precipitated rind also only revealed the presence of Al.

By cleaving the reacted "crystals" parallel to the (0 1 0) cleavage plane we were able to obtain excellent cut-away views of unaltered albite cores surrounded by massive reaction rims. Fig. 8 is a 20× SEM image of a crystal reacted at 300°C at *pH* 2.36 for 62 h. The rind consists of massive ($\sim\frac{1}{2}$ mm thick), non-epitaxially grown crystalline boehmite. This SEM image shows some of the best evidence to date that massive rims of secondary phases can precipitate on hydrothermally altered feldspars. Previous related studies, such as those by Wyart et al. [26], Tchoubar and Oberlin [27] and Tchoubar [28] only found evidence for noncoherent epitaxial occurences of boehmite and other secondary phases, such as kaolinite. Fig. 9 is an SEM image at 5000× showing bladed, outward radiating crystal masses of boehmite. Note the large amount of interconnected void space. On this criterion alone, it is probable that the rate of aqueous diffusion of product ions would not be hindered by the presence of a porous precipitate. Fig. 10 is a 5000× image of the albite–boehmite interface. The linearity of the interface was verified by many SEM traverses. From the apparent direction of growth of the boehmite crystals towards the retreating albite interface, it is possible that the degree of Al supersaturation and rate of crystal nucleation may be highest at the boehmite–albite interface. This suggests that Al precipitation occurs at the interface, rather than at the outside surface of the reaction rim. It should be noted, however, that other occurences of boehmite crystals at the interface displayed a much more random orientation, similar to that shown in fig. 9.

Mass balance calculations were made to evaluate whether or not the deficit in the Al concentrations from the packed bed experiments could be ac-

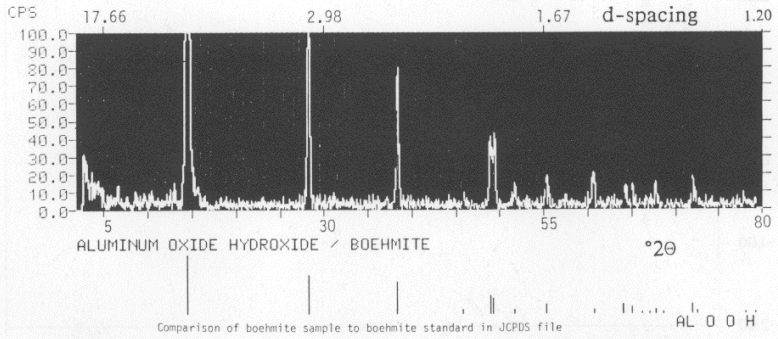

Fig. 7. X-ray diffraction pattern of the alternation rind formed on an albite cleavage fragment that was run in a flow experiment at 300°C at *pH* 2.36 for 62 h. The pattern reveals that the rind is composed of crystalline boehmite (AlO(OH)).

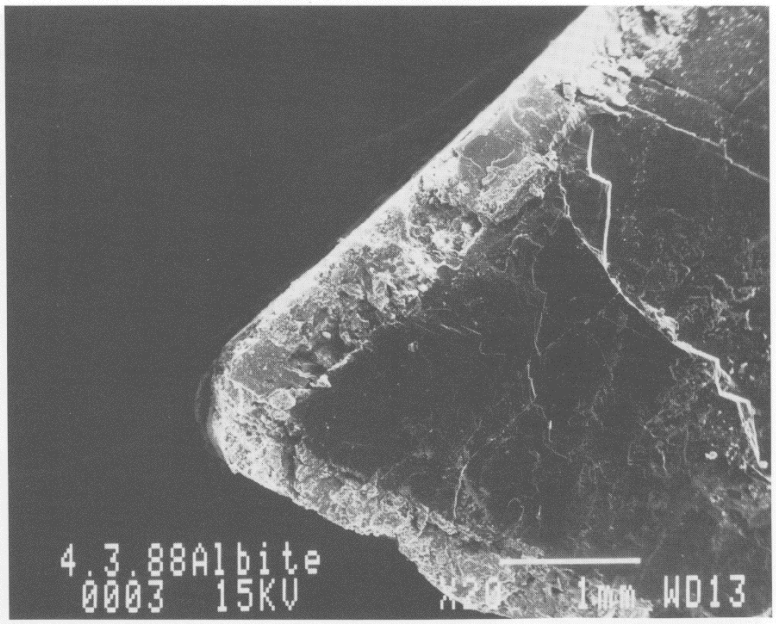

Fig. 8. A 20× SEM image of an albite fragment surrounded by a 1/2 mm thick reaction rim of crystalline boehmite. The rind formed after contact with a flowing solution of *pH* 2.36 at 300°C for 62 h.

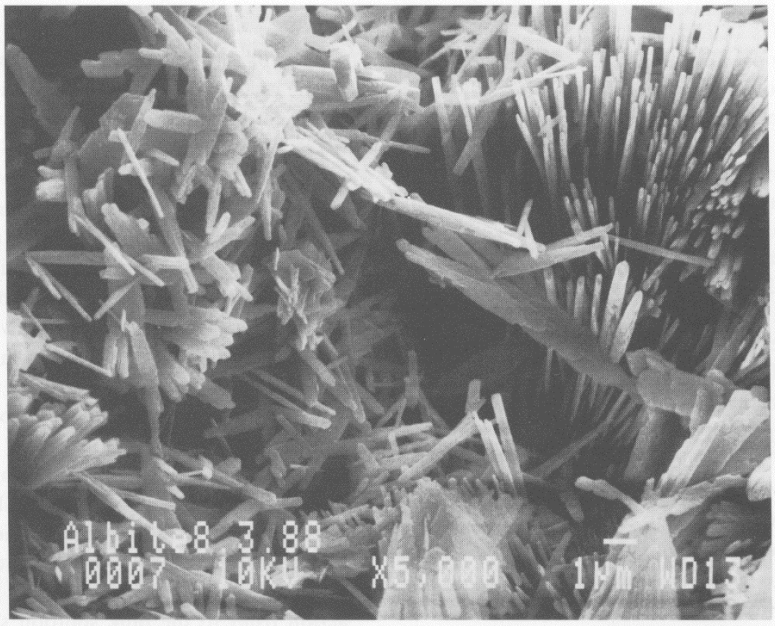

Fig. 9. A 5000× SEM image of the rind shown in fig. 8. Note the high degree of porosity among the bladed crystal masses of boehmite.

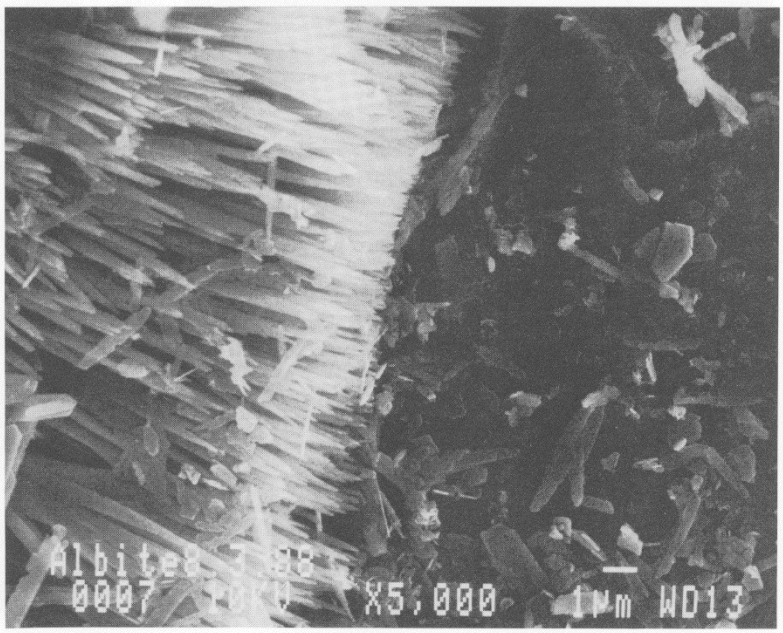

Fig. 10. A 5000× SEM image of the interface between boehmite and albite. Note how the tips of the boehmite crystals point in the direction of the interface, indicating possible growth in the direction of the retreating albite core.

counted for by precipitation of Al as boehmite. The molar deficit of Al in the effluent solution of the packed bed experiment at pH_{in} 2.46 and 300°C, over a period of 62 h, was used to predict the number of moles of boehmite which theoretically could precipitate. This value was compared to calculations based on a rind formed during an experimental run where a single crystal was exposed to a pH_{in} 2.36 solution at 300°C for 62 h. The number of moles of observed boehmite rind was found to be approximately 3× higher than the value predicted from the packed bed experiments. The discrepancy between the two calculations can be attributed to uncertainty in the dimensions and porosity of the rind as well as the fact that the *pH* of the single crystal experiment was 1/10 of a unit lower than the packed bed experiment. It is also inherently difficult to compare both results because of the positive axial *pH* gradient in the packed bed experiments. Since the solution *pH* increases as a function of axial length, preferential precipitation of boehmite will occur at the upstream end (inlet) of the reactor. Precipitation at the inlet end of the reactor seems counterintuitive, since the solubility of boehmite increases at both acid and basic *pH*'s. However, the rate of Al hydrolysis is also greatest at low, acidic *pH*'s, leading to Al oversaturation and precipitation of boehmite. Therefore, if the axial *pH* gradient were to be taken into account, the predicted amount of boehmite precipitation should increase. If all of these factors are considered, then it seems plausible that the results would agree quite closely. Even if these correction factors are not applied, it is reasonable to postulate that the negative release ratios of Al/Si can be accounted for by the precipitation of boehmite.

It was discussed earlier that the large percentage of interconnected void space seen in SEM images of the boehmite phase would preclude the possibility of it acting as a diffusional barrier to the outward flux of product species (such as Na and Si) from the reaction front to the bulk solution surrounding each

grain. This is based on the fact that diffusion of products in an aqueous medium is significantly faster than the intrinsic rate of structure breakdown. Another point to consider is that the molar volume ratio of boehmite to albite is 0.195. According to the empirically derived Pilling–Bedworth rule (Gomes and Dekeyser [29]), when the molar volume ratio of precipitate to reacting substrate is less than unity, then the precipitate will not be diffusionally limiting with respect to the flux of product ions. The reproducibility results (figs. 5 and 6) offer additional proof that secondary precipitates do not diffusionally inhibit ion fluxes. If we consider the fact that the values of the negative release ratios for the same conditions (pH_{in} 5.7) did not change over the course of several hundred hours, and if it is assumed that the rate of Al precipitation remained constant under equivalent conditions, then it seems very likely that the outward flux of Si was not influenced by the formation of a boehmite reaction rim. If this would not have been the case, then the release ratios would have increased as a function of rim. In summary, it is apparent that two critical properties of secondary precipitates, the porosity and the molar volume ratio (precipitate/reactant), determine whether or not a secondary phase acts as a diffusional barrier to product species released during dissolution. The precipitation of massive boehmite does not seem to affect the release rate of Si species into solution. In the next section, we will discuss why this does not necessarily hold true for Na ions.

4.2. Incongruency and sodium retention above 100°C

Most of the release ratios at temperatures exceeding 100°C have means centered approximately around −0.1 log units on the release ratio scale. This corresponds to a 25% linear deficit in the solution Na/Si ratio. This far exceeds the estimated 5–10% analytical error in the data at these elevated temperatures. If the results were to be solely attributed to suboptimal analytical accuracy and/or precision, then the scatter should be symmetric about the congruency line. This is clearly not the case. Thus, the deficiency in Na must be a real phenomenon. From the X-ray diffraction pattern (fig. 7), we already noted that boehmite was the only phase present in the reaction rim. An electron microprobe backscattered image of the rim also failed to show evidence for more than one phase. Saturation index calculations based on the computer code EQ3NR (Wolery [30]) indicated that boehmite was the only phase supersaturated in the reactor core. These lines of evidence show that Na is not being retained as a discreet secondary phase.

Preliminary near surface studies of hydrothermally altered albite utilizing XPS (X-ray photoelectron spectroscopy) facilities at the Center for Materials Research at Stanford University led to the hypothesis that sorption of Na ions may be the cause for the negative Na/Si release ratios. The XPS spectra generally showed that the near surface of hydrothermally reacted albite crystals was depleted in Na. However, whenever boehmite crystals had precipitated on the surface (as revealed by SEM), the spectra yielded an enhanced Na signal, indicating a slight degree of enrichment of Na, either at the albite surface or within the boehmite. This effect was only noted in those cases where precipitates had formed. Unfortunately, from the XPS data alone we were not able to resolve the question of which phase was sequestering the Na ions.

Broken bonds and other atomic disturbances affect the electroneutrality of mineral structures such that most minerals have a net surface charge. The nature of the charged surface is both an inherent property of the mineral as well as the surrounding aqueous environment. In order for surface electroneutrality to be maintained, non-specific electrostatic adsorption of ions on the charged surface will occur, resulting in the formation of an electrical double layer about the surface. The double layer provides a "reservoir" for counterion adsorption. There are many models which treat the spatial distribution of charged species within the double layer (for a review, the reader is referred to Parks [31] or Stumm and Morgan [32]). The potential at a solid–liquid interface exponentially dereases to zero in the bulk solution. The net charge that a surface will carry is dependent on the amphoteric nature of adsorbed surface MOH (M = metal) groups as well as the adsorption of aqueous metal hydroxo ($M^{z+}(OH)_n^{z-n}$) complexes (Parks [33], and references therein). The solution *pH* at which a surface has a net zero charge

is called the zero point of charge (ZPC). At solution *pH*'s less than the ZPC the net surface charge will be positive, and conversely, at *pH*'s above the ZPC the surface will carry a net negative charge. Thus, Na ions which have become detached from the structure will be electrostatically attracted to surfaces carrying a net negative charge. The albite–boehmite interface and the boehmite rind are the two available surfaces for adsorption, the ZPC's of each are approximately 2.0–2.4 and 7.7–9.4, respectively [31,33]. Based on the given values of the ZPC's, Na adsorption theoretically should take place at the albite–boehmite interface for all solutions with *pH* less than 7.7 to 9.4, whereas at higher *pH*'s adsorption could occur on the interface as well on the boehmite crystal surfaces.

In order to test the idea that Na ions were being adsorbed in an amount equal to the deficit of Na in the output solution, we applied the Gouy–Chapman electrical double layer model to the albite–boehmite interface and calculated the total adsorption density. For the calculations we used the evaluated form of the integral of the concentration profile (see ref. [31], p. 248). The major uncertainties in the calculations were due to the estimation of the surface area and the value used for the potential drop across the mobile part of the double layer. These points aside, the value calculated for the total amount of Na adsorbed agreed with the solution data within a factor of approximately 3. The calculations suggest that for a given set of conditions, there is approximate agreement between the Na deficit in solution and the calculated amount of Na that could be adsorbed in an electrical double layer. However, these calculations do not consider time as a variable. The adsorption of Na into the double layer is instantaneous with respect to the time scale of the experiments. The reproducibility results (figs. 5 and 6) show that the degree of Na deficiency remains the same for equivalent experimental conditions over a period of several hundred hours. For the deficiency to remain constant, there would have to be a concomitant increase in the total adsorption density of Na in the electrical double layer. The most obvious way to satisfy this condition would be for the surface area to increase over time. At present it is difficult to ascertain whether the change in surface area of the albite interface during dissolution would be sufficient to allow for the adsorption density to increase.

The boehmite crystals could possibly be the other environment for adsorption of Na ions. Here the capacity to serve as a substrate for adsorption would steadily increase with time since the boehmite rind continuously grows in thickness and volume. As mentioned before, the measured ZPC of synthetic boehmite ranges from 7.7 to 9.4. However, Parks [33] has noted that naturally formed boehmite can have a ZPC $\leqslant 2$. If this were the case, then the boehmite undoubtedly could serve as an environment for adsorption. With the continual addition of few surface area, the amount of Na adsorbed would remain fairly constant over time, thus corroborating the constant release ratio findings.

4.3. Incongruency and preferential release of Al and Na at 25 and 100°C

As figs. 2 and 3 show, the release ratio values for Al/Si and Na/Si at 25 and 100°C show different behavior than their counterparts at temperatures above 100°C. The first major difference is the degree of scatter. At 25°C, the scatter in the Na/Si and Al/Si release ratios spans up to 3 log units. The degree of scatter in the data is at least an order of magnitude less at 100°C, especially with respect to the Na/Si data. The high degree of scatter in the data for both sets of release ratios can be attributed in large part to a low degree of analytical accuracy and precision inherent in the measurements. At low temperatures, the rates of dissolution were low enough such that the effluent solution concentrations of Al, Na and Si were often in the range of only a few tens of ppb.

Despite the high degree of scatter in the data, the other major difference in release ratio behavior is still apparent. The means of the Na/Si release ratios are positive at 25 and 100°C, and for Al/Si, they are only positive at 25°C. The positive release ratios cannot simply be attributed to suboptimal analytical accuracy and/or precision. If this were the case, then the data should be spread more or less symmetrically about the zero congruency line. This is evidently not the case.

The influence of surface fines also cannot be invoked to explain these results. The presence of surface fines has been given attention in the literature as a major reason for initially high rates of dissolution. The higher rates of dissolution have been at-

tributed to their higher degree of solubility. Nevertheless, increased rates of dissolution should not be a factor leading to the prevalence of positive release ratios. It may be possible to presume that the initial high rate of dissolution is characterized by the preferential release of Na and Al with respect to Si. However, over the course of several hundreds of hours of dissolution any surface fines which were initially present would have been completely dissolved away (as revealed by SEM). Complete dissolution would imply that these particles would only contribute stoichiometric ratios of product ions to the solution. Figs. 5 and 6 show that the positive release ratios are reproducible after several hundreds of hours of dissolution. Based on this reasoning, the role of surface fines can be discounted as a source for the positive release ratios. A similar argument can be applied to the initial presence of mechanically disturbed sites on the surfaces of grains. If these sites contributed to incongruent dissolution, then surface annealing after contact with 300°C solutions should have occured over the duration of the experiments, thus diminishing any possible role disturbed surfaces may have had with respect to incongruency.

The most likely explanation for positive incongruency at low temperatures is that the output solutions were not sampled under steady state conditions. This indicates that not enough time was allowed for equilibrium to be established between the packed mineral bed and the flowing solutions at 25°C, and for the case of Na, also at 100°C. Thus, these results provide information on the processes involved during the initial phases of dissolution when dissolution is incongruent. Past studies (see, for example, [6,7,9] and references therein) have shown that the initial stages of feldspar hydrolysis are characterized by the exchange of protons for alkalis, resulting in an alkali depleted, Si-rich zone at the near surface. The initial phase of incongruent dissolution gradually evolves into a steady state, congruent dissolution process. The time required for the onset of steady state conditions at 25°C is still not clear. Results from [6,7] suggest tens of hours, whereas data from [9] indicate that several hundred hours may be required for the attainment of steady state conditions.

The results from these packed bed experiments confirm that the initial phases of hydrolysis are marked by the rapid exchange of protons for both Na and Al in the structure. Thus, atoms in the albite structure that are considered to be both network modifiers and network formers are subject to preferential leaching from the lattice, leaving behind a depleted zone consisting of (possibly hydrated) Si and O. The existence of leached layers has been subject to debate because XPS studies have, until now, failed to detect depletion of Na and Al to depths greater than a few Ångströms [10–12]. However, our preliminary XPS results do, in fact, show that under conditions similar to those used for the packed bed experiments, depletion of Na and Al extends several tens of Å into the sructure (details on our XPS results will be forthcoming).

Chou and Wollast [6,7] postulate that the formation and subsequent collapse of depleted zones enriched in Si can be effected by instantaneously changing the input solution from an acidic to a basic medium. Unfortunately, the scatter in our data preclude extracting similar observations. It does seem likely, however, that another reason for some of the scatter in the data at low temperatures, for any given input *pH*, is attributable to sampling at various stages of the initial dissolution period.

5. Conclusions

The release ratio results from our packed bed experiments suggest that the data are representative of two distinct phases of dissolution. The low temperature data (25°C for Al/Si; 25 and 100°C for Na/Si) describe the initial phase of incongruent dissolution. The positive incongruency of the release ratios denotes that Na and Al are preferentially leached from the near surface of the albite structure. Since the rate of hydrolysis is a function of temperature, at temperatures above 100°C steady state conditions were achieved in our experiments. Current interpretations of the leached layer dissolution model suggest that steady state conditions are attained when a critical thickness of the leached layer is reached, such that the rate of diffusion of product ions through the leached layer equals the rate of structure breakdown (see [6,7] and references therein). The release ratios obtained from our data taken at elevated temperatures indicated that the effluent solution in nearly

all cases was deficient in Al and Na with respect to Si. In the case of Al, massive precipitation of boehmite led to the negative release ratios. The rate of hydrolysis was apparently most rapid at low *pH*'s, resulting in the greatest degree of Al precipitation as well as the most negative release ratios. The release ratios of Na/Si at elevated temperatures also indicated that Na was selectively retained; however, the degree of retention was much less than for Al. The non-specific electrostatic adsorption of Na ions either at the albite–boehmite interface, or within the boehmite rim, is a possible mechanism for producing negative release ratio values. If the effects due to the precipitation of Al and the adsorption of Na are taken into account, then the data support the conclusion that albite dissolves congruently at steady state conditions.

From the non-steady state results at low temperatures, the release ratio data support the hypothesis that the initial dissolution process is controlled by the formation of a leached layer. However, there also exists evidence that dissolution is controlled by surface reactions. This means that hydrolysis takes place at specific surface sites which have high surface strain energies. These sites occur where dislocations, microfractures or other imperfections in the near surface of the structure intersect the surface. Fig. 11 quite graphically illustrates that a surface control mechanism must be operative. The etch pits were formed on an Amelia albite grain reacted at *pH* 2.46 at 25°C for 80 h. Berner et al. [20] pointed out that evidence such as this is contrary to the leached layer model. Reconciling the two hypotheses calls for a model with surface reactions constrained to localized areas on the surface which would be most prone to attack by hydrolysis reactions, coupled to the formation of leached layers at these sites. As pointed out in [20,23], leached layers need not be continuous either spatially or with respect to depth. Thus, it seems that our data suggest that initial phases of dissolution are controlled *both* by surface reactions and the formation of localized leached areas.

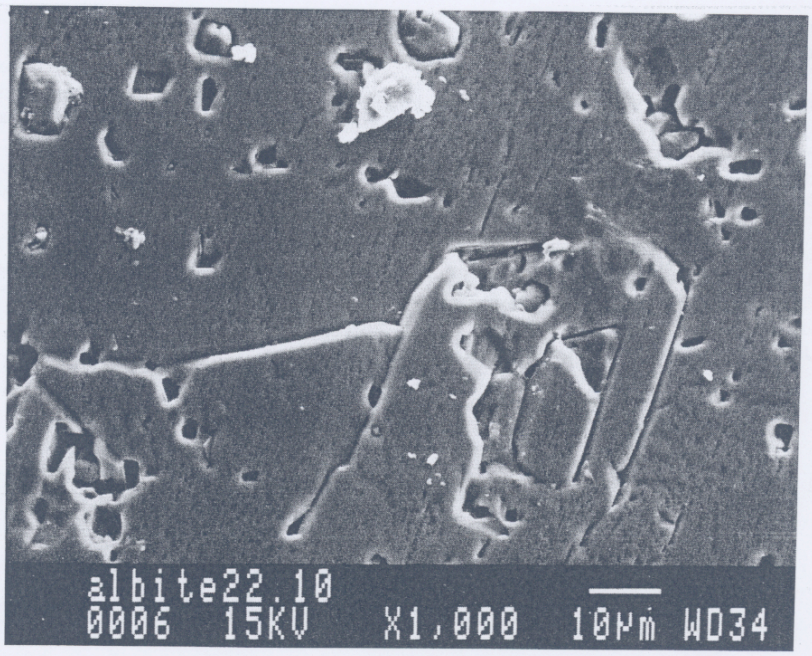

Fig. 11. Well developed etch pits on an albite fragment run at *pH* 2.46 at 25°C for 80 h at a rate of 1.6 ml/min in a flow reactor. The presence of etch pits indicates that dissolution occurs preferentially at certain surface sites.

Acknowledgement

We would like to thank Maria Borcsik for her assistance with the chemical analyses; Ted Forseman, George Rose, and Charles Kulick for machining and electrical circuitry expertise; Elaine Lenk for assistance with the SEM; Cameron Davidson and Susan Swapp for microprobe analyses. Preliminary XPS work was done at the Center for Materials Research, Stanford University; for this we thank Carrick Eggleston and Michael Hochella Jr. for their time and support. Helpful discussions with George Parks are acknowledged. Bear McPhail and Carrick Eggleston gave helpful editorial advice. Financial support for this project was from N.S.F. grants (to D.A.C.) EAR-8218726 and -8407651. D.A.C. also gratefully acknowledges financial support from the Shell Companies Foundation.

References

[1] C.W. Correns and W. von Engelhardt, Chem. Erde 12 (1938) 1.
[2] R. Wollast, Geochim. Cosmochim. Acta 31 (1967) 635.
[3] Y. Tsuzuki and K. Suzuki, Geochim. Cosmochim. Acta 44 (1980) 673.
[4] R.M. Garrels and P. Howard, in: Proc. Sixth National Conf. Clays and Clay Minerals, Oxford, England, 1957, ed. A. Swineford (Pergamon Press, New York, 1957) p. 68.
[5] T. Pačes, Geochim. Cosmochim. Acta 37 (1973) 2641.
[6] L. Chou and R. Wollast, Geochim. Cosmochim. Acta 48 (1984) 2205.
[7] L. Chou and R. Wollast, Am. J. Sci. 285 (1985) 963.
[8] R. Wollast and. L. Chou, in: The chemistry of weathering: NATO ASI Series, C 149, ed. J.I. Drever (Reidel, Dordrecht, The Netherlands, 1985) p. 75.
[9] G.R. Holdren Jr. and P.M. Speyer, Am. J. Sci. 285 (1985) 994.
[10] R. Petrović, R.A. Berner and M.B. Goldhaber, Geochim. Cosmochim. Acta 40 (1976) 537.
[11] G.R. Holdren Jr. and R.A. Berner, Geochim. Cosmochim. Acta 43 (1979) 1161.
[12] P.C. Fung, G.W. Bird, N.S. McIntyre, G.G. Sanipelli and V.J. Lopata, Nucl. Technol. 51 (1980) 188.
[13] M. Lagache, Bull. Soc. Franç. Miner. Crist. 88 (1965) 223.
[14] M. Lagache, Geochim. Cosmochim. Acta 40 (1976) 157.
[15] R.A. Berner and G.R. Holdren Jr., Geochim. Cosmochim. Acta 43 (1979) 1173.
[16] P. Aagaard and H.C. Helgeson. Am. J. Sci. (1982) 237.
[17] H.C. Helgeson, W.M. Murphy and P. Aagaard, Geochim. Cosmochim. Acta 48 (1984) 2405.
[18] W.E. Dibble Jr. and W.A. Tiller, Geochim. Cosmochim. Acta 45 (1981) 79.
[19] R.A. Berner and J. Schott, Am. J. Sci. 282 (1982) 1214.
[20] R.A. Berner, G.R. Holdren Jr. and J. Schott, Geochim. Cosmochim. Acta 49 (1985) 1657.
[21] G.R. Holdren Jr. and P.M. Speyer, Geochim. Cosmochim. Acta 51 (1987) 2311.
[22] K.G. Knauss and T.J. Wolery, Geochim. Cosmochim. Acta 50 (1986) 2481.
[23] L. Chou and R. Wollast, Geochim. Cosmochim. Acta 49 (1985) 1659.
[24] J. Posey-Dowty, D.A. Crerar, R. Hellmann and C.D. Chang, Am. Mineral. 71 (1986) 85.
[25] J.D.H. Stickland and T.R. Parsons, Canada Fish. Res. Board Bull. 167 (1972) 65.
[26] J. Wyart, A. Oberlin and C. Tchoubar, CR Acad. Sci. Paris, 256 (1963) 554.
[27] C. Tchoubar and A. Oberlin, J. Microscopy 2 (1963) 415.
[28] C. Tchoubar, Bull. Soc. Franç. Miner. Crist. 88 (1965) 483.
[29] W.P. Gomes and W. Dekeyser, in: Treatise on solid state chemistry, Vol. 4, Reactivity of solids, ed. N.B. Hannay (Plenum Press, New York, 1976) p. 61.
[30] T.J. Wolery, UCRL-53414 Lawrence Livermore Nat. Lab., Livermore, CA (April, 1988).
[31] G.A. Parks, in: Chemical oceanography, eds. J.P. Riley and G. Skirrow, 2nd Ed. (Academic Press, London, 1975) 241.
[32] W. Stumm and J.J. Morgan, Aquatic chemistry, 2nd Ed (Wiley, New York, 1981) p. 610.
[33] G.A. Parks, Chem. Rev. 65 (1965) 177.